

Protein Folding Activity of the Ribosome is involved in Yeast Prion Propagation

Marc Blondel¹, Flavie Soubigou^{1§}, Justine Evrard^{1§}, Phu hai Nguyen^{1,3}, Naushaba Hasin^{2,4}, Stéphane Chédin⁵, Reynald Gillet⁶, Marie-Astrid Contesse¹, Gaëlle Friocourt¹, Guillaume Stahl⁷, Gary W. Jones^{2,8}, Cécile Voisset^{1*}.

Supplementary information

Supplementary Figures Legends

Figure S1. (A) Diagram of 40S:60S ratio modification in *Itv1Δ* or *yar1Δ* mutants (right) compared to *WT* (left). *Itv1Δ* and *yar1Δ* mutants contain more free 60S subunits in the cytoplasm than *WT* strain due to defective cytoplasm translocation of 40S subunits. **(B)** Survival of *WT*, *Itv1Δ*, *yar1Δ*, *hsp104Δ*, *Itv1Δ/hsp104Δ* and *yar1Δ/hsp104Δ [psi-]* cells used in **Fig. 1D and 1E** after specified post-heat-shock incubation periods.

Figure S2. (A) Cells from red halos surrounding filters on which 6AP or GA was loaded (**Fig. 2A**) were streaked on drug-free YPD medium. Cells surrounding filters on which DMSO and GdnHCl were loaded were used as negative and positive controls, respectively. **(B)** Read-through levels in *Itv1Δ* and *yar1Δ [psi-]* strains compared to *WT [psi-]* strain ¹. **(C)** The permeability of [*PSI⁺*] *WT*, *Itv1Δ* and *yar1Δ* strains was analyzed. Cells were spread on YPD medium and small filters were placed on the agar surface. 10 nmoles (filters 2, 3, 4) and 20 nmoles (filters 1, 5, 6, 7) of ethanol (filter 1), menadione (filters 2 and 5), Ifenprodil (filters 3 and 6) and chlorhexidine (filters 4 and 7), that are toxic for yeast cells, were applied to each filter. The non-growing halos caused by the four toxic compounds spotted on *WT*, *Itv1Δ* and *yar1Δ* strains had similar diameters, indicating that the reduced sensitivity to 6AP, GA and GdnHCl of [*PSI⁺*] prion in *Itv1Δ* and *yar1Δ* mutants was not due to a global change in membrane permeability. **(D)** [*PSI⁺*] *Itv1Δ* and *yar1Δ* strains were crossed with a *WT [psi-]* strain and the four cells issued from the diploid sporulation were tested for their sensitivity to 6AP and 6APi. The transmission of prion was faithful from *Itv1Δ* and *yar1Δ [PSI⁺]* cells to [*psi-]* *WT* cells, indicating that the resistance to prion curing in *Itv1Δ* and *yar1Δ* was not due to modification of the prion strain. **(E)** Polysome profiles of *WT [PSI⁺]* strain transformed by an empty plasmid (left panel) or by a plasmid allowing Bms1p overexpression (OE, right panel). Cells overexpressing Bms1p display an impoverishment in 40S subunits as well as an elevated level of free 60S subunits compared to the strain transformed by the empty plasmid. 60S:40S ratio was 1.48 for *WT* strain transformed by the empty vector p416-GAL1, and 2.69 for *WT* strain overexpressing Bms1p. The y axis shows arbitrary units. **(F)** *WT [PSI⁺]* cells transformed by an empty plasmid (left panels) or by the plasmid allowing Bms1p overexpression (right panels) were spread on glucose- (- panels) or 2% galactose-containing medium (+ panels) supplemented with 200 μM GdnHCl. Small filters were then placed on the agar surface and various

amounts of 6AP and GA were applied to each filter, except for the top left filter where DMSO was added (negative control). The size of the red halos is proportional to the efficiency of $[PS^+]$ curing. **(G)** [URE3] stability was evaluated by scoring [ure3-0] colonies appearing from [URE3] cells, as a percentage of total cells for *WT* and *yar1Δ* strains. Bar height represents the mean; *t*-test: $**P < 0.001$ versus to *WT* cells grown on YPD. **(H)** Polysome profiles of *WT* and *yar1Δ* [URE3] strains showing that *yar1Δ* mutant strain displayed elevated levels of free 60S subunits, as well as an impoverishment in 40S subunits compared to *WT* strain that is particularly poor in 60S subunits.

Figure S3. (A) $[PS^+]$ is less efficiently cured by GdnHCl in PFAR-enriched strains than in *WT* strain. $[PS^+]$ *WT*, *Itv1Δ* and *yar1Δ* strains were spread on YPD medium. Small filters were then placed on the agar surface and various amounts of GdnHCl were applied to each filter, except for the top left filter where DMSO was added (negative control). The size of the red halos is proportional to the efficiency of $[PS^+]$ curing. **(B)** Model of the interplay between protein folding activities of Hsp104p and ribosome in modulating $[PS^+]$ propagation. We propose a model of how Hsp104p and PFAR may sustain together the propagation of $[PS^+]$ (**panel a**). **Panel b** - $[PS^+]$ propagation is similarly affected by enrichment in Hsp104p by heat shock or overexpression (upper left, ^{a2,3}) or PFAR by 60S enrichment (upper right, ^b(this paper, **Fig. 2**)) or by inhibition of Hsp104p by GdnHCl (lower left, ^{c4}) or PFAR by 6AP (lower right, ^{d5}). **Panels c & d** - On this model for Hsp104p and PFAR interplay, reducing the activity of one could be compensated by enrichment of the activity of the other.

Figure S4. Summary of data presented in **Figure 4 (A)** and in **Figure 5 (B)** in the light of the model shown in **Figure S3B**.

Supplementary Table

Table S1 – primers used to create mutant strains and snoRNAs

Primer name	Primer sequence (5' to 3')
Deletion primers	
LTV1-F	GTATTT CAAAGA CTTTAA GGGGAA TATAAA AAGCAC GAAGCG GATCCC CGGGTT AATTAA
LTV1-R	GTACTT GTAATG TAGGTG CTTTCT CATCTC ATTCTA CTCCTG AATTCG AGCTCG TTAA
YAR1-F	TATTC CAAATA GAAAAA AAAAAT CTACAT ATACGC AGATCG GATCCC CGGGTT AATTAA
YAR1-R	ATTACG GCTTTT ATTCCA CGAAGA AAACAA GCTCTT TACTGA ATTCGA GCTCGT TAAAC
HSP104-F	AAAGAA ATCAAC TACACG TACCAT AAAATA TACAGA ATATCG GATCCC CGGGTT AATTAA
HSP104-R	ATTCTT GTTCGA AAGTTT TAAAA ATCACA CTATAT TAAAGA ATTCGA GCTCGT TAAAC
RPL8A-F	CATTGCTTACCCTCTATTATCACATCAAACAACAACTAATTCGAACGGATCCCCGGGTTAATTAA
RPL8A-R	ATFAAAAAATAAATTTTTTATGCAAAATTTTCATTTTCAATGAATTCGAGCTCGTTTAAAC
LTV1-Fbis	GAATAT TATGAG CATCTA AATC
LTV1-Rbis	GCATCA ATGCAT TCTAGG C
YAR1-Fbis	GTGGTA ATATCA CCATGA ACG
YAR1-Rbis	GCATTT CTGCTG GTTCCA TC
HSP104bis-F	GAACGT CAAATT ATATCA CAG
HSP104bis-R	ATTATT CACAG CAAGAT GAAC
RPL8Abis-F	ATTACTATTCCAGTTGTCAG
RPL8Abis-R	CTTAAAAGGTTATTTAAGGTC
snoRNA guide sequences and analysis primer	
BLO-38	ATACATTAATAGATCTCCAAGAAACTACGC
snoRNA-U2954	GGGTTAGACCGTC
snoRNA-U2862	TTTTTGATTCTTCG
snoRNA-G2863	TTTTGATTCTTCGA
snoRNA-U2873	TCGATGTCGGGCTCT
snoRNA-C2876	ATGTCGGCTCTCC
snoRNA-U2932	CCACTAATAGGGAA
snoRNA-G2957	TTTAGACCGTCGTG
RT Q-PCR primers	
25S-F	AGACCGTCGCTTGCTACAAT
25S-R	ATGACGAGGCATTTGGCTAC
18S-F	TTGTGCTGGCGATGGTTCA
18S-R	TGCTGCCCTCCTTGGATGTG
Actin-F	ATGGTCGGTATGGGTCAAAAA
Actin-R	TTCCATATCGTCCCAGTTGGT

Supplementary References

- 1 Stahl, G., Bidou, L., Rousset, J. P. & Cassan, M. Versatile vectors to study recoding: conservation of rules between yeast and mammalian cells. *Nucleic acids research* **23**, 1557-1560 (1995).
- 2 Helsen, C. W. & Glover, J. R. Insight into molecular basis of curing of [PSI⁺] prion by overexpression of 104-kDa heat shock protein (Hsp104). *J Biol Chem* **287**, 542-556, doi:10.1074/jbc.M111.302869 (2012).
- 3 Wickner, R. B. *et al.* Amyloids and yeast prion biology. *Biochemistry* **52**, 1514-1527, doi:10.1021/bi301686a (2013).
- 4 Liebman, S. W. & Chernoff, Y. O. Prions in yeast. *Genetics* **191**, 1041-1072, doi:10.1534/genetics.111.137760 (2012).
- 5 Tribouillard-Tanvier, D. *et al.* Protein folding activity of ribosomal RNA is a selective target of two unrelated antiprion drugs. *PLoS ONE* **3**, e2174 (2008).

Figure S1

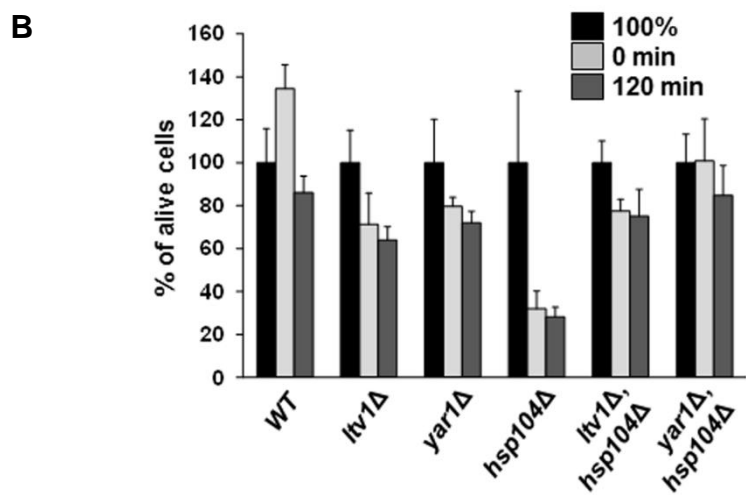
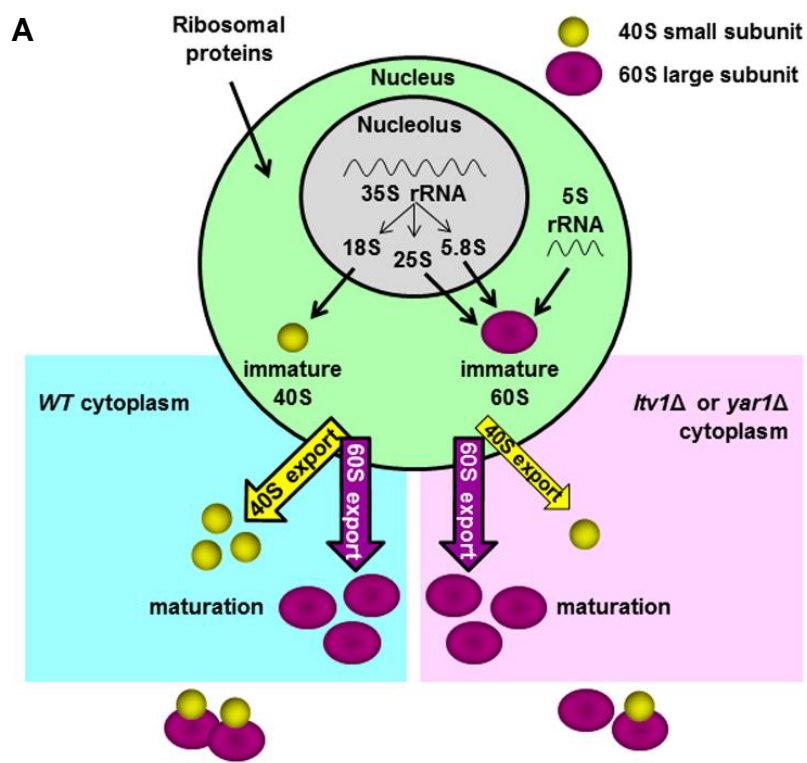


Figure S2

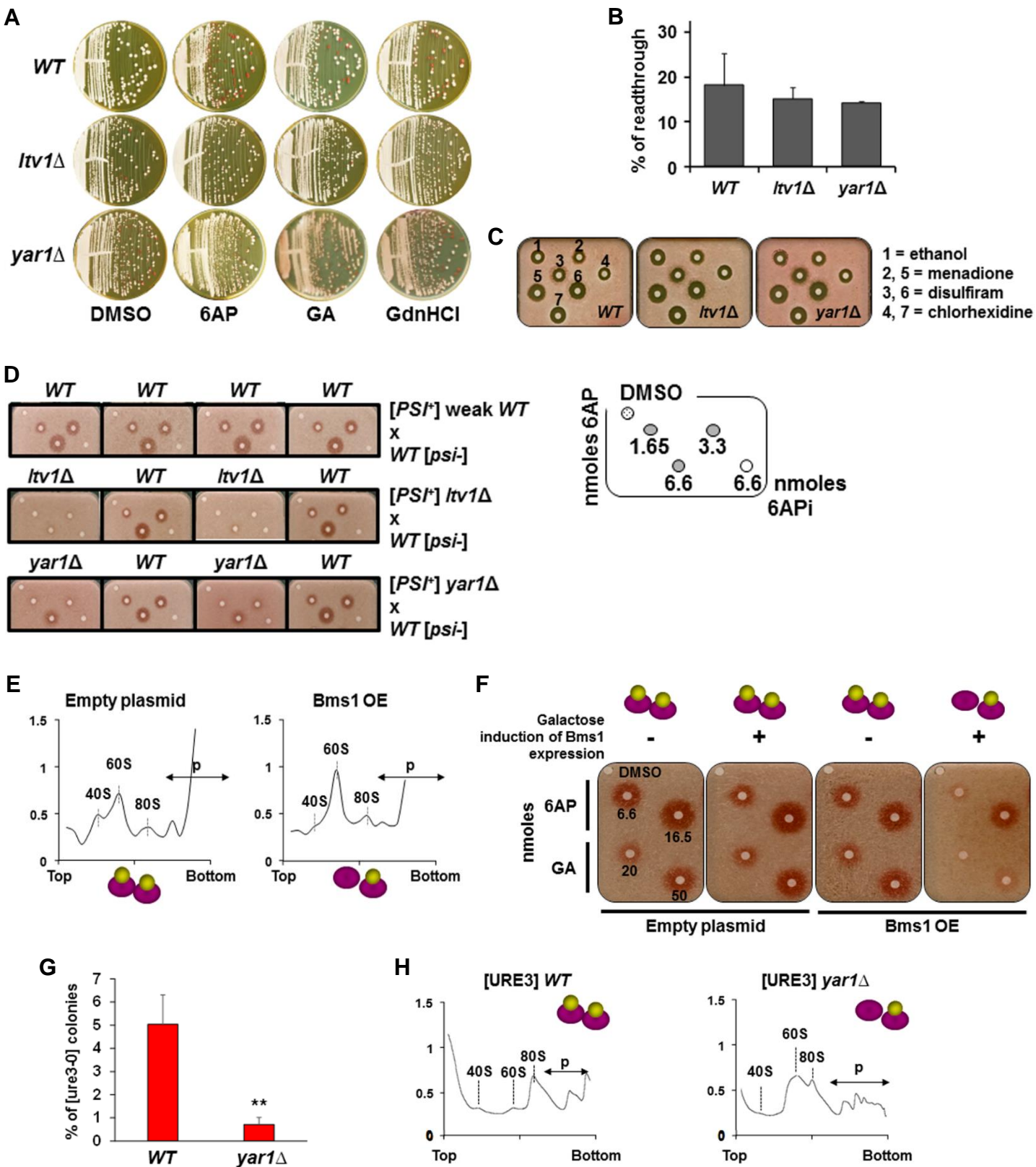


Figure S3

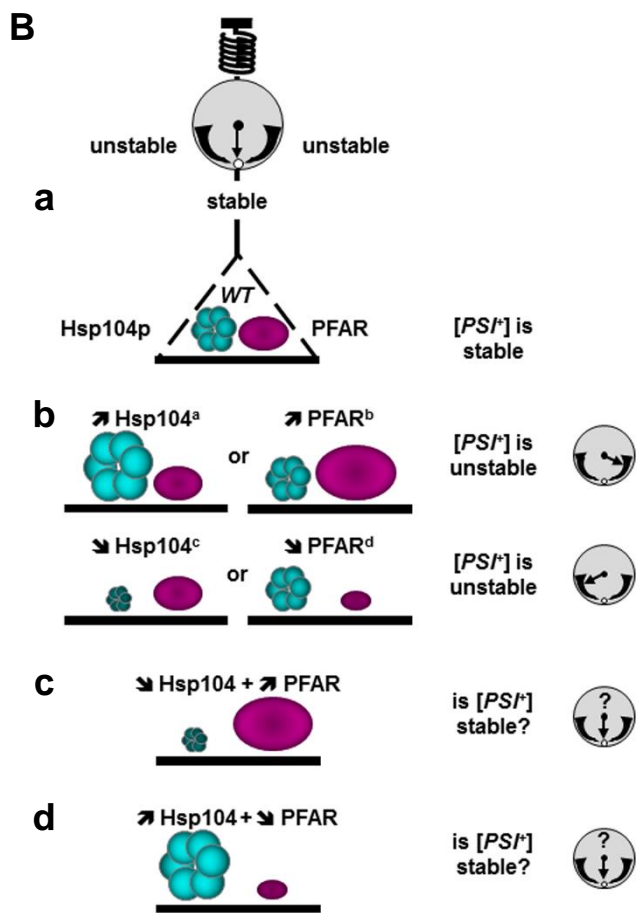
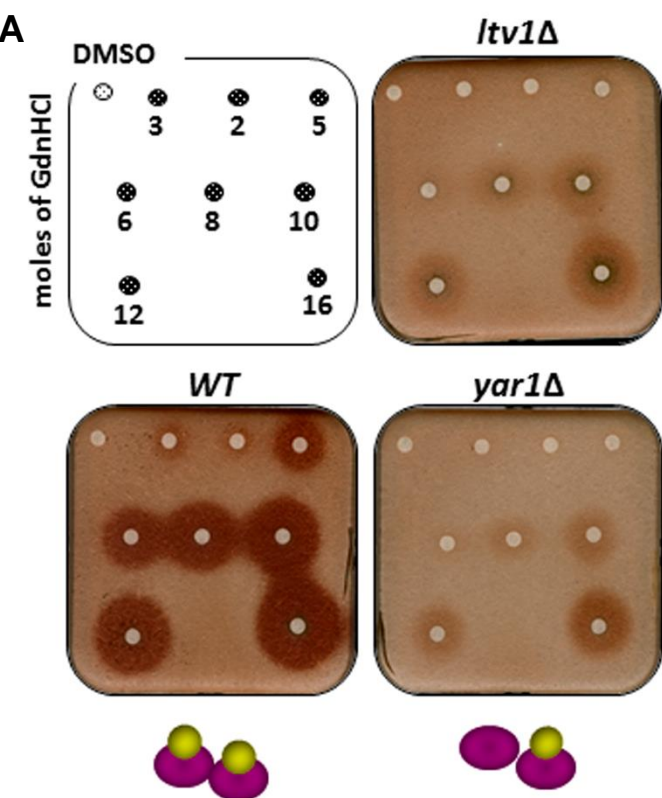


Figure S4

